Limnol. Oceanogr., 52(3), 2007, 1179–1187

Optical effect on the nitracline in a coastal upwelling area

Dag L. Aksnes[1]
Department of Biology, University of Bergen, N-5020 Bergen, Norway

Mark D. Ohman
Scripps Institution of Oceanography, University of California–San Diego, La Jolla, California 92093-0218

Pascal Rivière
LEMAR, Institut Universitaire Européen de la Mer, 29280 Plouzané, France

Abstract

The transport of nitrate into the euphotic zone is an important regulator of primary production. This transport is facilitated by physical processes that involve the depth and the steepness of the nitracline, but transport is complicated by the dynamical nature of the euphotic zone. Here we derive an analytical model that predicts two optical effects of the euphotic zone on the nitracline: the nitracline depth should vary inversely with light attenuation for downwelling irradiance, and the nitracline steepness should be directly proportional to light attenuation. We show that observations of nitrate and Secchi depth, which have been obtained over 21 yr in the coastal upwelling region off Southern California (CalCOFI area), are consistent with these predictions. Chlorophyll *a* measurements also indicate an optical signature in the nitracline: while the amount of chlorophyll correlated poorly with the nitracline depth, the nitracline depth correlated strongly with the optical effect of chlorophyll, and the nonlinear nature of this relationship was consistent with the model prediction. These optical effects on the nitracline may involve positive feedback mechanisms with phytoplankton production that have implications for interpretation and modeling of primary production.

The vertical transport of nitrate into the euphotic zone is an important regulator of ocean productivity (Eppley et al. 1979; Lewis et al. 1986). The euphotic zone is the depth zone at which light intensity is sufficient to support net photosynthesis, but this zone is commonly calculated as the depth to which a certain percentage of the surface photon flux penetrates (Ryther 1956). The depth of the euphotic zone is not fixed, but rather varies as a function of actual surface radiance, attenuation properties of the water, and its dissolved and particulate constituents, as well as physiological properties of the producers. Thus, the statement that the vertical transport of nitrate into the euphotic zone regulates phytoplankton production can be turned around: phytoplankton production is regulated by how far the euphotic zone extends into the oceanic nutrient pool. These statements are not contradictory but simply underscore the common knowledge that phytoplankton growth is generally exposed to two opposing resource gradients: light supplied from above and nutrients supplied from below. Neither of these resource gradients is static, and the dynamics of both influence rates and patterns of production. Based on a modeling study, Huisman et al. (2006) demonstrated that the two gradients, together with sinking of phytoplankton, could generate oscillations and chaos in numerical simulations of oceanic deep chlorophyll maxima (DCM). Letelier et al. (2004) found that changes in surface light and the water column light attenuation had a large effect on DCM and nitracline dynamics in the North Pacific Subtropical Gyre.

Lewis et al. (1986) specified an analytical model to explain vertical nitrate distributions in the oligotrophic ocean. In such ocean areas there is a deep euphotic zone characterized by low attenuation of downwelling irradiance because of a low phototrophic biomass and reduced concentrations of other particulate and dissolved attenuating substances. In coastal areas, light attenuation tends to increase because of higher nutrient input to the euphotic zone leading to higher phototrophic biomass (Lewis et al. 1988), but it also tends to increase because of other particulate and dissolved light-attenuating substances (Conversi and McGowan 1994; Højerslev et al. 1996; Sosa-Ávalos et al. 2005). Such processes shoal the euphotic zone depth, which in turn is likely to affect the nitracline.

Here, we derive a simple analytical model whereby the two nitracline properties, depth and steepness, are described as a function of vertical nitrate transport and nitrate consumption. We specifically derive predictions of how the two nitracline properties relate to light attenuation. These predictions are compared with observations from the upwelling area off the coast of Southern California (CalCOFI area). Although the CalCOFI database does not contain extensive time series of optical properties, a large number of Secchi disc measurements are available. As pointed out by Lewis et al. (1988), global observations of Secchi depth provide a very useful record of

[1] Corresponding author (dag.aksnes@bio.uib.no).

Acknowledgments

We thank Marlon R. Lewis and John Marra for helpful suggestions.

This work was sponsored in part by the Leiv Eriksson Fellowship 169601 from the Norwegian Research Council (D.L.A), an LTER Fellowship (P.R.), and the California Current Ecosystem LTER site.

Table 1. List of symbols. Dimensionless quantities are indicated by d.l.

Symbol	Explanation	Unit
a	Nitrate uptake rate coefficient	s^{-1}
c	Beam attenuation coefficient	m^{-1}
C_{av}	Average chlorophyll *a* (Chl *a*) concentration above Secchi depth	mg Chl *a* m^{-3}
E	Normalized irradiance	d.l.
K	Light-attenuation coefficient for downwelling irradiance	m^{-1}
K_{Chl}	Light attenuation for downwelling irradiance due to chlorophyll	m^{-1}
K_z	Vertical turbulent diffusivity	$m^2\ s^{-1}$
l	Coefficient of the relationship between Secchi depth and K	d.l.
N	Normalized nutrient concentration	d.l.
n	Nutrient concentration defining the nitracline depth	d.l.
O	Number of observations	
t	Time	s
w	Upwelling rate	$m\ s^{-1}$
w'	Scaled upwelling rate ($w' = w/a$)	m
z	Depth	m
Z_n	Nitracline depth (depth where $N = n$)	m
Z_s	Secchi depth	m
Z_{12}	Nitracline depth (depth where nutrient concentration is 12 μmol L^{-1})	m
α_n	Nitracline steepness (at depth where $N = n$)	μmol L^{-1} m^{-1}
α_{12}	Nitracline steepness (at nitracline depth, Z_{12})	μmol L^{-1} m^{-1}
ψ	$= w' \ln n$	m

the variability in optical characteristics and production of the world oceans. Such observations have also proven useful in the analyses of variability in large marine fish stocks (Aksnes 2007). In addition to the Secchi observations, extensive CalCOFI chlorophyll measurements permit analysis of the importance of self-shading in shaping the nitracline.

Our use of an equilibrium model for the nitracline and of the Secchi disc to assess the optical regime has limitations. In particular, this methodology restricts us from analysis of nitracline dynamics on short temporal and spatial scales. Our approach, however, is suitable for interpretation of nitracline dynamics on seasonal and interannual scales as well as for the interpretation of persistent nitracline variations that are observed along coast-to-offshore transects (Eppley et al. 1978, 1979).

A simplified nitracline model

Nitrate (N) dynamics in the water column are commonly described in terms of uptake, vertical transport, and mixing, thus (Table 1):

$$\frac{\partial N}{\partial t} = -\text{uptake} - w\frac{\partial N}{\partial z} + K_z\frac{\partial^2 N}{\partial z^2} \qquad (1)$$

where w is the upwelling rate and K_z is the vertical turbulent diffusivity. More generally, a regeneration term as well as nitrogen fixation should also be included, but these processes are not addressed here. Similar to the steady-state analyses of Lewis et al. (1986) and Fennel and Boss (2003), we consider the nitracline as an equilibrium between nitrate consumption and vertical supply (by the assumption $dN/dt = 0$). To obtain predictions on how nitracline properties specifically relate to light attenuation for downwelling irradiance, in the absence of turbulent diffusion, we set $K_z = 0$. This means that the nitracline steepness predicted from our model is governed by light attenuation only. The additional effect of turbulent diffusion will tend to decrease the nitracline steepness, and this effect is addressed below in our comparison between predictions and observations.

We define the normalized nondimensional nitrate concentration (N) of Eq. 1 as the ambient concentration divided by a characteristic concentration of the deep nitrate reservoir so that $0 < N \leq 1$. We also consider the normalized ambient light at depth z, $E = \exp(-Kz)$, where K is the light-attenuation coefficient of downwelling irradiance. This implies that daily and seasonal variations in surface radiance will not be accounted for in our model but that this quantity can be characterized by an average.

We assume that the uptake term of Eq. 1 is determined by ambient light and the nitrate concentration. Hence, we acknowledge the presence of nitrate consumers (i.e., the phototrophic biomass), but we consider them to be catalysts that facilitate conversion of nitrate into organic substances in the presence of light. Accordingly, and similar to the findings of Lewis et al. (1986), we describe nitrate removal at depth z as a linear function of ambient light and nitrate; uptake $= aEN = ae^{-Kz}N$ where a is a coefficient characterizing the nitrate uptake of the phototropic biomass. Insertion of this quantity in Eq. 1, and assuming that $K_z = 0$ and $dN/dt = 0$, will yield $wdN/dz = -ae^{-Kz}N$. Separation of variables and integration yields:

$$\ln N = \frac{1}{Kw'}e^{-Kz} \qquad (2)$$

where $w' = w/a$ (m) is the vertical velocity scaled against the biological consumption rate. This equation predicts how the vertical distribution of nitrate (i.e., the nitracline) is affected by the vertical transport of nitrate and downwelling irradiance as determined by the optical depth Kz. For a given

w' we see from the example in Fig. 1A that Eq. 2 predicts nitracline shoaling of 70–80 m for an increase in light attenuation from 0.05 to 0.10 m^{-1}. Such increased light attenuation will commonly be governed by enhanced phytoplankton production as a result of increased vertical nitrate transport (e.g., upwelling characterized by w) but can, especially in coastal regions, also be related to nitrate discharges from land runoff and to dissolved and particulate light-attenuating substances other than phytoplankton.

The hypothesized relationship between the nitracline depth and the Secchi depth—We make use of Eq. 2 to derive the expected relationship between the nitracline depth and the Secchi depth (Z_S). We first define the nitracline depth (Z_n) as the depth at which the normalized nitrate concentration is equal to n. In principle, n can be any normalized concentration between 0 and 1. Insertion of $N = n$ for $z = Z_n$ in Eq. 2 yields the expected relationship between the nitracline depth and the attenuation coefficient of downwelling radiance:

$$Z_n = \frac{-\ln(K\psi)}{K} \tag{3}$$

where $\psi = w' \ln n$. Now we make use of the relation between the Secchi depth and the optical parameters, $Z_S \propto (K + c)^{-1}$, where c is the beam attenuation coefficient (Preisendorfer 1986). Beam attenuation is the sum of absorbance and scattering, but K also depends on these two inherent properties. The tight relationship between K and c implies that the Secchi depth can be expressed as $Z_S = lK^{-1}$, where l reflects the $c:K$ ratio and the Secchi disc coupling constant defined by Preisendorfer (1986). The value $l = 1.7$ (after Poole and Atkins 1929) has often been applied, but no specific value is assumed here (unless for the illustration purpose in Fig. 1B). Substitution of K with Z_S in Eq. 3 yields:

$$Z_n = -l^{-1} Z_S \ln(l Z_S^{-1} \psi) \tag{4}$$

This nonlinear relationship between nitracline and Secchi depth is illustrated in Fig. 1B (solid line). Here we have also indicated the fit of a straight line to simulated data containing errors in the nitracline depths and the Secchi depths (Fig. 1B, dotted line). For data containing errors in the determination of these two depths, it is not possible to discriminate a linear from a nonlinear fit, and we therefore applied linear regression in the analyses of the CalCOFI data. It should be noted that the validity of the linear approximation should be checked for particular applications because it depends on the actual parameter values. In particular, if a small nitrate concentration (n) is chosen to represent the nitracline depth, a linear approximation might not be valid. Similarly, very shallow Secchi depths (less than a few meters), and thereby shallow nitracline depths, also tend to strengthen the nonlinear relationship between them.

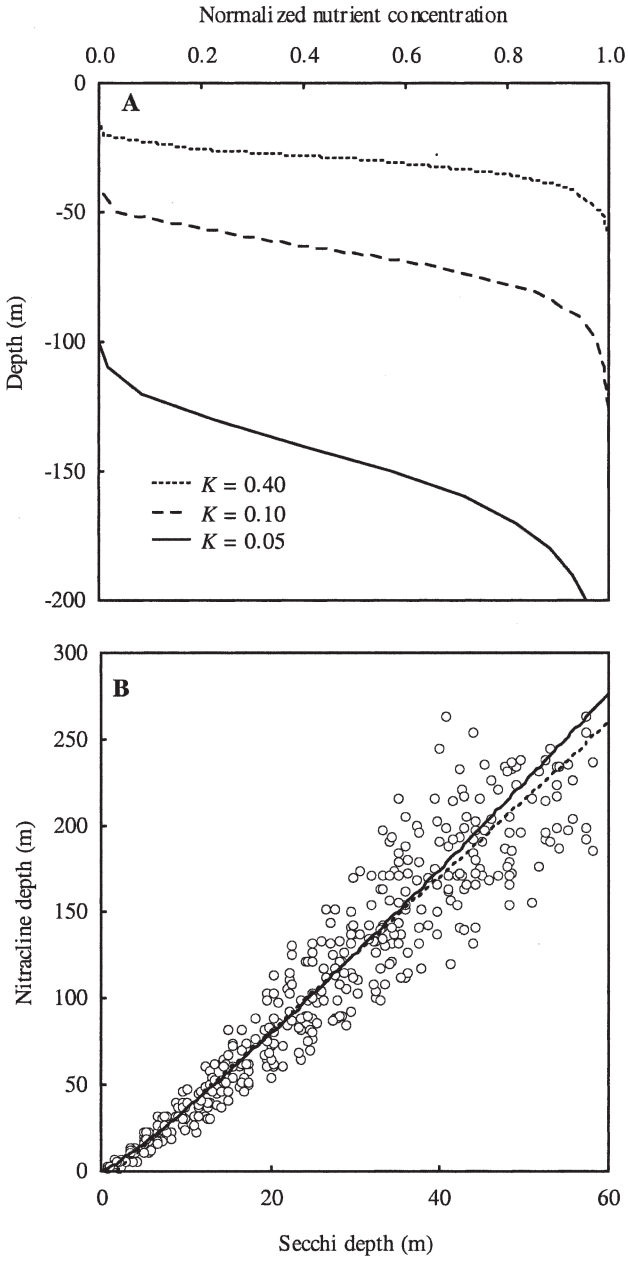

Fig. 1. (A) The nitracline for three different light-attenuation coefficients for downwelling radiance (K), as predicted from Eq. 2. The scaled rate for upward transport of nitrate was constant for the three scenarios ($w' = -0.02$ m). (B) The solid line represents the relationship between the nitracline depth and the Secchi depth, as calculated from Eq. (4), assuming $\psi = -0.02 \ln 0.5$ and $l = 1.7$ (Poole and Atkins 1929). The data points also represent calculated nitracline and Secchi depths, but where random rectangular errors within ±20% were added. The dotted line represents a linear fit to these simulated values. This linear fit cannot be discriminated from the parametric nonlinear line (solid).

The hypothesized relationship between the steepness of the nitracline and the Secchi depth—From Fig. 1A it can be seen that Eq. 2 predicts that the nitracline becomes steeper with increased light attenuation. At the nitracline depth (Z_n) where $N = n$, we now define the associated nitracline steepness according to $\alpha_n \equiv dN/dz = nw'^{-1} \exp(-KZ_n)$. By

insertion of the expression for Z_n (Eq. 3) this simplifies to:

$$\alpha_n = \text{const} \times K, \tag{5}$$

and if nitracline steepness is expressed as function of the Secchi depth ($Z_S = lK^{-1}$):

$$\alpha_n = \frac{\text{const} \times l}{Z_S} \tag{6}$$

where const $= -n \ln n$ is determined by the normalized nitrate concentration that has been chosen to characterize the nitracline depth. Thus, this equation predicts that the steepness of the nitracline should be proportional to the light attenuation and to the reciprocal Secchi depth.

We now have a model that predicts how the nitracline depth and its steepness are affected by the light attenuation for downwelling irradiance (Eqs. 3 and 5) and that also predicts how the nitracline properties are expected to distribute as a function of observed Secchi depths (Eqs. 4 and 6). We will use the CalCOFI data to test these predictions. Erosion of the nitracline by turbulent mixing, which has not been accounted for here, will reduce the steepness and might, for a particular data set, hide the optical signature expressed in Eqs. 5 and 6.

Methods

CalCOFI data—For the period from 1984 to 2004 observations of Secchi depth, nitrate concentrations, chlorophyll *a* (Chl *a*) concentrations, and vertically integrated Chl *a* were obtained from the CalCOFI database (www.calcofi.org). Observations obtained between the latitudes 35°15′ and 30°30′ and east of longitude 124°45′ were used. This corresponds approximately to CalCOFI sampling lines 77 to 93. Only stations containing both Secchi readings (i.e., daytime) and nitrate measurements were applied in the analyses. This gave O = 2,187 pairs of observations for the entire time period. Very few nutrient measurements were taken in 1984, so this year was omitted when annual averages were calculated.

To analyze the data according to a coast–offshore gradient, we organized the observations into subareas that followed the contour of the Southern California coast. These subareas consisted of 0.5° × 0.5°–sized geographical cells, and the width of each subarea corresponded to approximately 50 km. Hence, the first subarea was approximately within 50 km of the coast, the second extended 50–100 km from the coast, etc. We defined the innermost three subareas (i.e., within approximately 150 km off the coast) as the inshore area.

Calculation of the nitracline depth and steepness—In the analyses of the CalCOFI data, the nitrate measurements were not normalized, but this has no consequence for our analyses because the nitrate concentration is proportional to the normalized concentration. We have defined the nitracline depth, Z_{12}, as the first depth on a station that had a nitrate concentration of 12 μmol L^{-1}. This concentration is in the lower mid-range of the nitracline concentrations found in these waters, and it is within the range that was reported for the bottom of the euphotic zone by Eppley et al. (1978). Nitracline depth is often defined for lower nitrate concentrations, but our predictions are not sensitive to the particular definition of this depth. As noted earlier, the choice of a very low concentration tends to magnify the nonlinearity between nitracline depth and Secchi depth (Eq. 4), but our choice of 12 μmol L^{-1} is not affected by this.

Linear interpolation was used to identify nitracline depths located between sampling depths. At the nitracline depth we calculated the nitracline steepness; $\alpha_{12} = (N_2 - N_1)/(Z_2 - Z_1)$, where Z_2 is the first sampling depth that had a concentration larger than or equal to 12 μmol L^{-1} and where Z_1 is the previous sampling depth.

Optical transformation of chlorophyll—We calculated the chlorophyll contribution to the light attenuation for downwelling irradiance according to Morel (1988):

$$K_{Chl} = 0.121 C_{av}^{0.428} \tag{7}$$

where C_{av} is taken as the average chlorophyll concentration above the observed Secchi depth at a particular station.

Results

Nitracline versus Secchi depth at individual CalCOFI stations—First, we test whether the predicted optical signature can be detected in simultaneous observations of nitracline and Secchi depths (i.e., observations obtained at the same day and at the same station). We performed a linear regression analysis for all pairs of nitracline and Secchi depths observations available in the period from 1984 to 2004. The results presented in Fig. 2A are consistent with an approximate linear relationship but with appreciable scatter ($Z_{12} = 12.2 + 3.56 Z_S$; $r = 0.75$, $p < 0.01$, O = 2,187). The positive correlation between the nitracline steepness and reciprocal Secchi depth ($r = 0.37$) was also consistent with the expectation of Eq. 6 ($a_{12} = 5.5 Z_S^{-1}$; $p < 0.01$, O = 2,187) but also with appreciable scatter (Fig. 2B).

It was of interest to see how the amount of phytoplankton (i.e., vertically integrated Chl *a*) related to the depth of the nitracline (Fig. 2C). The negative correlation ($r = -0.33$, $p < 0.01$, O = 2,175, the lower number of observations here was due to missing chlorophyll measurements) was significant, but with a much lower coefficient of determination than the relationship observed for the nitracline versus Secchi depth (Fig. 2A). An optical transformation of the chlorophyll data according to Eq. 7, however, yielded a much higher correlation ($r = 0.81$; Fig. 2D). The nature of this relationship was consistent with the expectation of Eq. 3: A fit of the coefficient ψ in Eq. 3 gave $Z_{12} = -\ln(0.039 K_{Chl})/K_{Chl}$ ($p < 0.01$, $r = 0.81$, O = 2,175), where K_{Chl} was calculated according to Eq. 7. This relationship accounted for 66% of the variation in nitracline depth (Fig. 2D).

While the results in Fig. 2A represent what can be considered the daily relationship between the nitracline

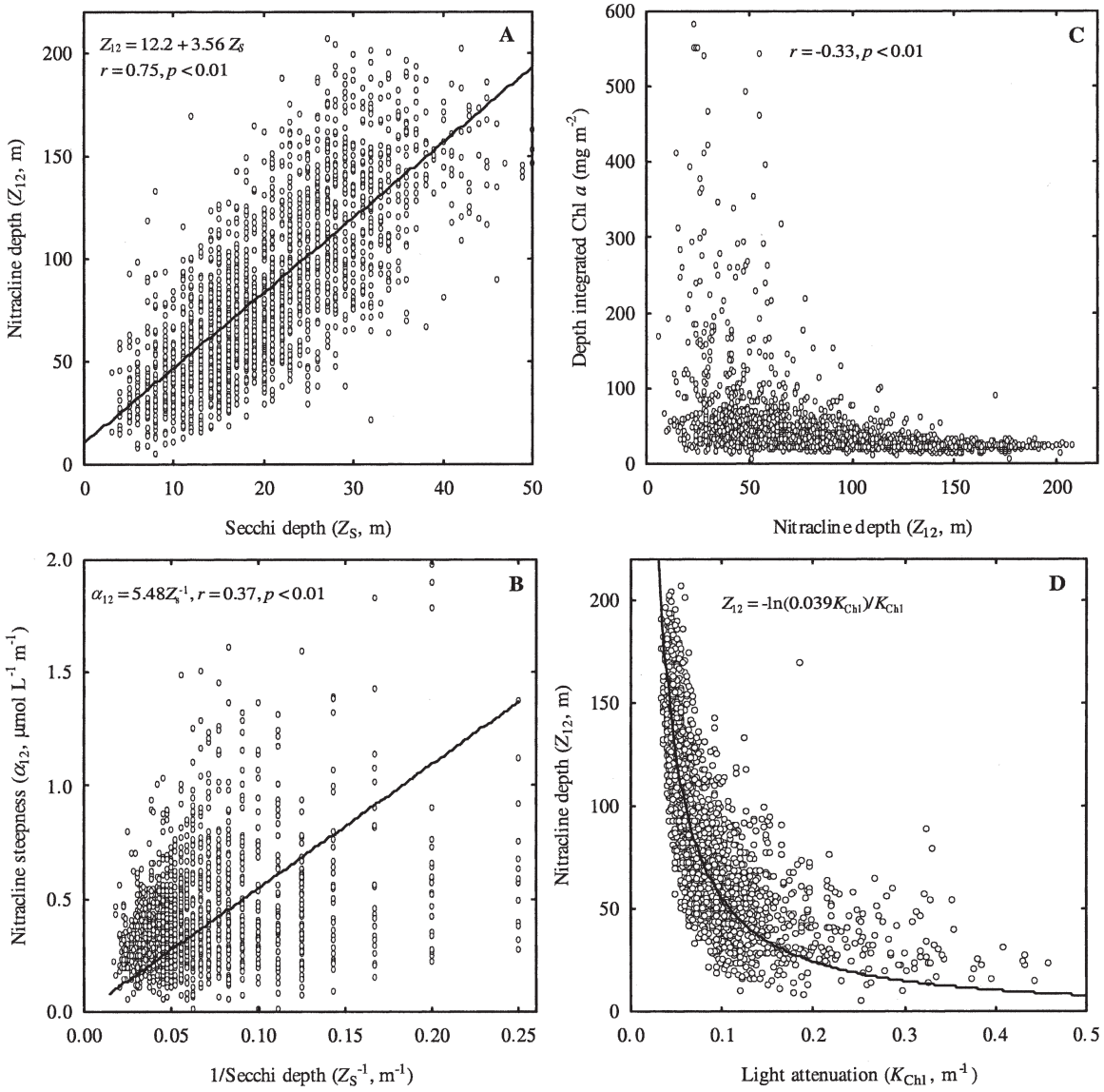

Fig. 2. (A) All pairs (O = 2,187) of observed nitracline depth and Secchi depth and (B) all pairs of observed nitracline steepness and reciprocal Secchi depth. (C) Vertically integrated Chl *a* versus nitracline depth. (D) Nitracline depth versus the chlorophyll component of the light-attenuation coefficient (K_{Chl}) that was calculated according to Eq. 7.

depth and the Secchi depth, we will now analyze this relationship for longer time scales (annual and seasonal averages) and at different locations in the cross-shore direction.

Interannual variations—In a linear regression, the interannual variations in Secchi depth accounted for 71% (r = 0.84, $p < 0.01$, O = 20) of the fluctuations in interannual nitracline depth (Fig. 3A). As predicted from Eq. 6, the fluctuations in the steepness of the nitracline were positively correlated (r = 0.54, p = 0.015, O = 20) with the fluctuations in reciprocal Secchi depth (Fig. 3B).

Seasonal variations—Within 150 km of the coast (inshore area) we observed concordant average seasonal patterns in nitracline depth and Secchi depth (Fig. 4A). In a linear regression the seasonal variations in Secchi depth accounted for 82% (r = 0.91, $p < 0.01$, O = 10) of the variations in nitracline depth, and variation in the reciprocal of the Secchi depth accounted for 79% (r = 0.89, $p < 0.01$, O = 10) of the variation in the nitracline steepness (Fig. 4B). We notice here that the seasonal cycle in the inshore area is characterized by a spring shoaling and a subsequent autumn deepening of the nitracline, and we will return to this feature in the Discussion section.

Variations in the cross-shore direction—A linear and concurrent deepening in both average Secchi and nitracline depth was also found when moving from nearshore toward the offshore (Fig. 5A), and a large part of the variance in the Secchi and nitracline depths in the CalCOFI area can be explained by the coast–ocean gradient. The deepening was

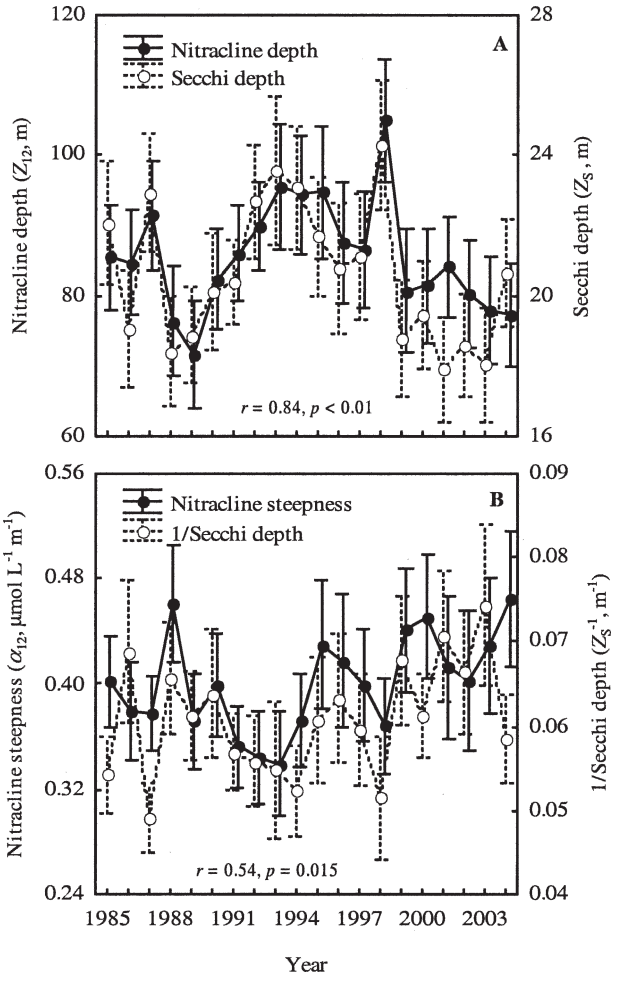

Fig. 3. (A) Annual variations in nitracline depth and Secchi depth. (B) Annual variations in nitracline steepness and reciprocal Secchi depth. The annual averages were calculated from all stations in the CalCOFI area where simultaneous Secchi depth and nitrate observations were taken. Error bars denote 95% confidence interval.

about 3 and 16 m per 100 km for the Secchi and nitracline depths, respectively. The nitracline deepening was accompanied by reduced steepness (α_{12}) (Fig. 5B), as predicted by Eq. 6.

While we observed a strong linear relationship between the nitracline and Secchi depths ($r = 0.99$, $p < 0.01$, $O = 15$; Fig. 6A), the observed relationship between the nitracline steepness and the reciprocal Secchi depth (Fig. 6B) deviated somewhat from the expectation of Eq. 6. While this equation predicts that a fitted straight line should pass through origin, the intercept with the y-axis of a linear regression analysis is positive (broken line in Fig. 6B; $a_{12} = 5.5Z_S^{-1} + 0.11$; $r = 0.92$, $p < 0.01$, $O = 15$). This indicates that the nitracline steepness as a function of reciprocal Secchi depth increases somewhat less than predicted from the optical effect expressed in Eq. 6 (the dashed vs. the solid line in Fig. 6B). Mixing is not accounted for in our model, and the effect of increased turbulent diffusion is reduced nitracline steepness. The discrepancy represented by the dashed and the solid lines in Fig. 6B might indicate intensified mixing at shallow nitracline depths (which correspond to high reciprocal Secchi depth) relative to deep nitracline depths (which correspond to low reciprocal Secchi depth).

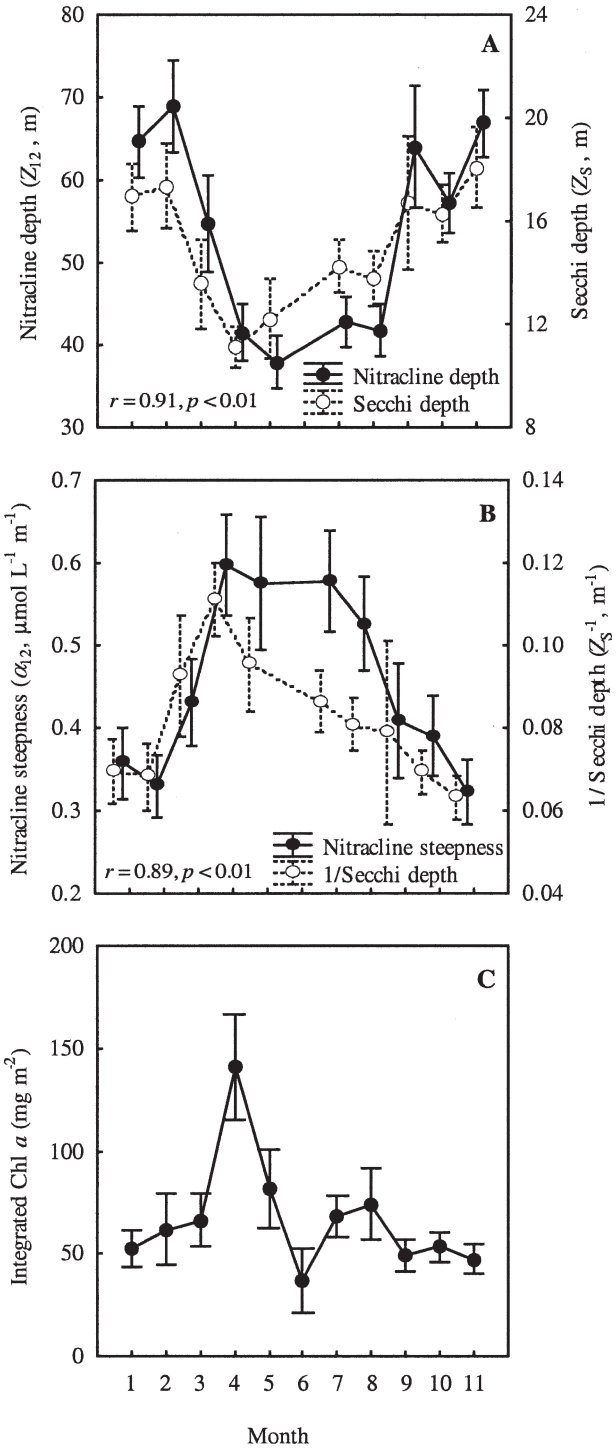

Fig. 4. (A) Average seasonal variations in nitracline depth and Secchi depth, (B) in nitracline steepness and reciprocal Secchi depth, and (C) in depth-integrated chlorophyll. Figures represent averages of all data in the inshore area (approximately within 150 km of the coast). Error bars denote 95% confidence interval.

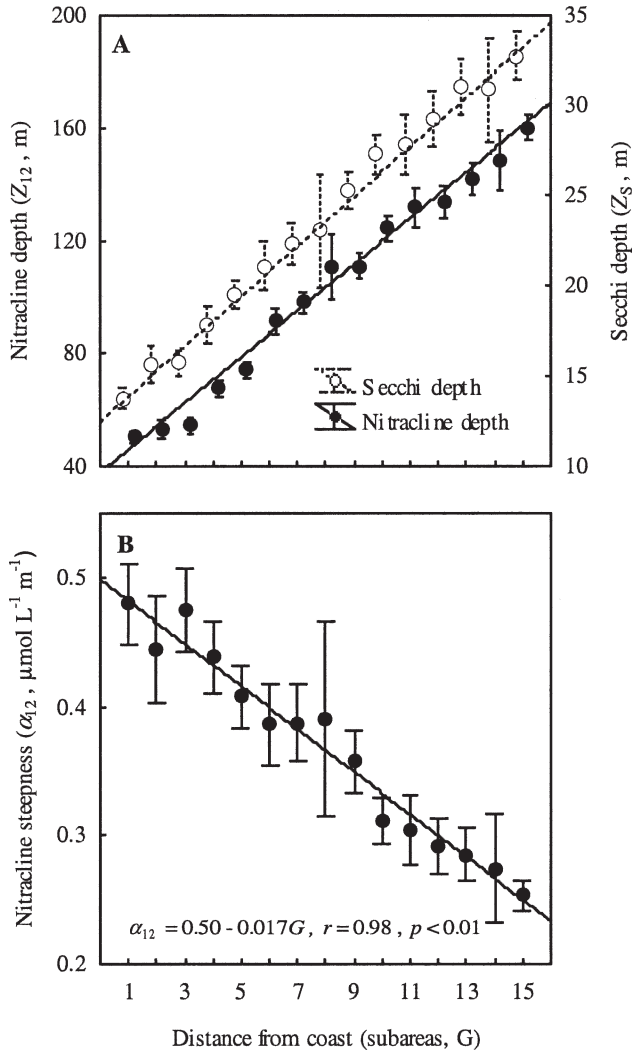

Fig. 5. Cross-shore variations in (A) nitracline depth and Secchi depth and (B) nitracline steepness when moving from the coast toward offshore. The averages are based on all available data in each of the 15 subareas that follow the coastline (*see Methods*). Each of the 15 subareas correspond to approximately 50 km. Error bars denote 95% confidence interval.

Discussion

The observed linear relationship between the nitracline and Secchi depths, the inverse relationship between the steepness of the nitracline and the Secchi depth, and the nonlinear relationship between the nitracline depth and the chlorophyll indicate an optical signature in the nitracline that is consistent with the theoretical predictions (i.e., Eqs. 2–6).

A shallow nitracline is likely to supply more nitrate into the euphotic zone than is a deep nitracline (Eppley et al. 1979), and a shallow nitracline will consequently give rise to a higher phototrophic biomass and a shallower Secchi depth. Thus, one might expect that the Secchi depth of the CalCOFI area merely passively reflected the depth of the nitracline via phytoplankton biomass. In that case we would have expected the correlation between phytoplankton biomass and nitracline depth (Fig. 2C) to be higher than the correlation between the Secchi depth and the nitracline (Fig. 2A). The opposite was the case. Unless the optical effect was important, it is very unlikely that the phototrophic biomass would respond to increased nitrate supply so that Secchi depth became linearly related to nitracline depth, and it is very unlikely that the light attenuation from the biomass would obey the prediction of Eq. 3 (i.e., $Z_n = -\ln(K\psi)/K$; Fig. 2D). This is exactly how the nitracline depth was expected to distribute according to the optical effect. But the clearest sign of an optical effect is the observed inverse relationship between the nitracline steepness and the Secchi depth. Equations 5 and 6 can explain why the observed nitracline becomes steeper as the nitracline shoals. This consistent pattern (Figs. 4–6) is harder to interpret in terms of turbulent diffusion and upwelling. This does not mean, however, that fluid dynamics are unimportant in shaping vertical nitrate distributions. It rather emphasizes how optics also affect nitracline dynamics.

How tight is the optical regulation of the nitracline for short timescales? Our study cannot give a definitive answer to this question. It shows that the variations in Secchi observations and the optically transformed chlorophyll measurements accounted for 56% and 66% of the variability in the nitracline depth, respectively (Fig. 2A,D). These estimates were obtained from observations conducted at the same station on the same day. A part of the unexplained variance is certainly due to errors in Secchi depth observations, in calculated nitracline depths, and in the calculated optical effect from chlorophyll measurements (according to Morel [1988]). Furthermore, our analysis did not account for seasonal variations in incoming radiance. Letelier et al. (2004) demonstrated a relatively large seasonal influence on the nitracline in the North Pacific Gyre, and in our analyses, any such effect would also have been included in the unexplained variance. This indicates that more than 56–66% of nitracline depth variation can be accounted for in studies designed to reveal day-to-day variations in the relationship between the nitracline and the light environment. Such studies would require replacement of the Secchi disc with radiometric measurements of the incoming radiance and light attenuation. Furthermore, a greater accuracy in the characterization of the nitracline depth and, in particular, nitracline steepness is needed.

Our methodology is more appropriate for analyzing optical effects on the nitracline for temporal averages exceeding the daily scale and spatial averages exceeding individual stations. Annual fluctuations, seasonal fluctuations, and the coast–ocean gradient all revealed empirical relationships between the nitracline and the Secchi depth that were consistent with predictions from the simple steady-state model. Depending upon which of these factors were used to organize the data, 71–99% of the variation in nitracline depth and 29–76% of the variation in steepness were accounted for by the Secchi observations.

Upwelling and reversed seasonal nitracline cycle—The spring shallowing and the subsequent autumn deepening of

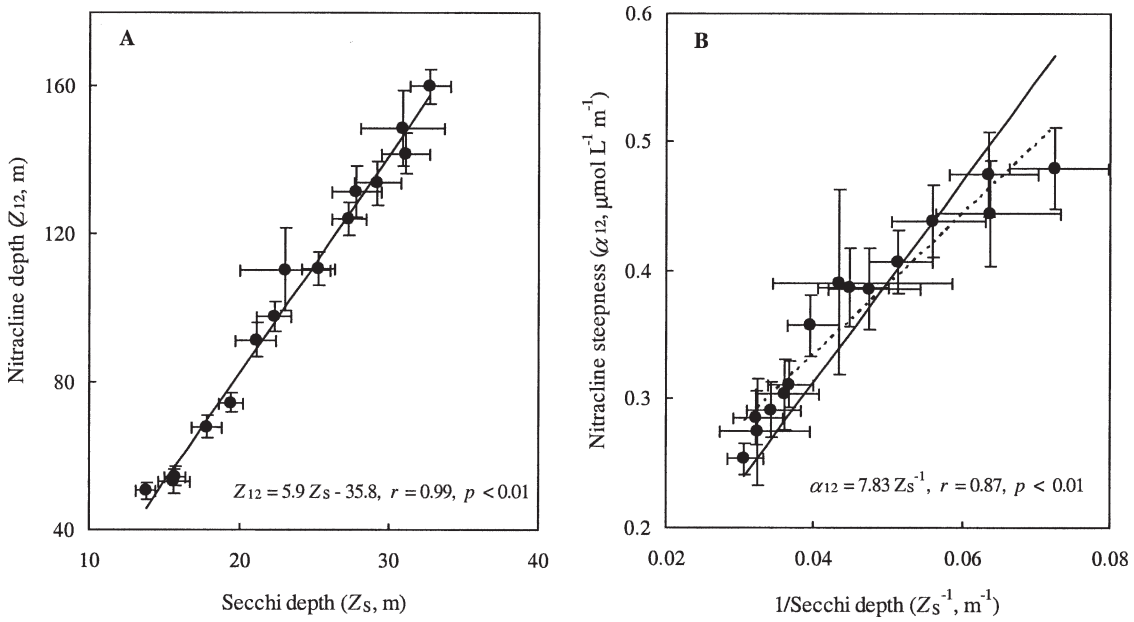

Fig. 6. (A) Linear regression between average nitracline and Secchi depths of the 15 subareas defined in Fig. 5. (B) Linear regression, forced through origin according to Eq. 6, between nitracline steepness and reciprocal Secchi depth. The broken line represents the fit from regular linear regression ($a_{12} = 5.5Z_S^{-1} + 0.11$; $r = 0.92$, $p < 0.01$).

the nitracline in the inshore area (Fig. 4A) are the reverse of what is generally observed in high-latitude systems and that described for the North Pacific Subtropical Gyre (Letelier et al. 2004). In these systems increased surface radiance and day lengths tend to deepen the euphotic zone and thereby the nitracline after a relatively intense but short spring bloom. On the contrary, the seasonal pattern in the CalCOFI inshore area showed a gradual phytoplankton biomass accumulation during spring (Fig. 4C) that was most likely fueled by upwelled nutrients (Eppley et al. 1978, 1979) at this time of the year (Lorenzo 2003). As indicated by the Secchi measurements, this biomass accumulation led to increased light attenuation (Fig. 4A) and thereby to a shallower euphotic zone, which, in addition to upwelling, tends to raise the nitracline further (e.g., a possible positive feedback).

In autumn the patterns are reversed, and our results indicate that the reversed seasonal nitracline cycle of the inshore area is governed by the concerted action of self-shading and seasonality in nitrate input rather than in the seasonal cycle in irradiance, as was observed in the North Pacific Subtropical Gyre (Letelier et al. 2004). Our results imply, however, that a shallowing nitracline per se cannot be taken as an unequivocal sign of increased upwelling. In general, phytoplankton accumulation can be caused by nitrogen sources other than those originating from the nitracline (e.g., from land runoff, atmospheric deposition, and nitrogen fixation), by advection of phytoplankton-containing layers, as well as by decreased phytoplankton sink terms, such as grazing and sinking rates. These interactions can potentially induce nitracline shoaling without any changes in physical transport rates. Furthermore, dissolved and particulate substances other than chlorophyll, as observed in connection with freshwater influence (Højerslev et al. 1996; Højerslev and Aarup 2002; Hamre et al. 2003) and other coastal/terrestrial influence (Conversi and McGowan 1994; Sosa-Ávalos et al. 2005), can contribute substantially to light attenuation and therefore shoal the euphotic zone and the nitracline independently of phytoplankton shading.

A potential positive feedback mechanism and suggestions for numerical modeling—The predicted optical effect on the nitracline implies a potential positive feedback mechanism. The nitracline is generally located deeper than the steepest temperature gradient in Southern California waters (Eppley et al. 1979), and such independent dynamics of the thermocline and the nitracline have also been observed and realistically simulated elsewhere (Aksnes and Lie 1990). The probability that nitrate enters the mixed layer, through the mixing barrier represented by the thermocline, will generally be higher for a shallow than for a deep nitracline. For example, if a pulse of nutrients to surface waters (e.g., through land runoff) causes a biomass-induced optical shoaling of the nitracline, more nitrate could at least temporarily fuel further growth. In principle, all processes and substances that enhance light attenuation, such as reduced grazing, biomass originating from human nutrient discharges, yellow substances from river runoff, advection of surface waters, etc., might potentially initiate a temporally positive feedback. The actual dynamics will depend on a number of factors that obviously cannot be explored by a steady-state model but that would require numerical simulations. Nevertheless, our results emphasize the importance of accurate representation of underwater optics in simulation models of ocean productivity. This applies in particular to coastal areas receiving light-attenuating substances other than chlorophyll. Inaccurate representa-

tion of light attenuation is likely to cause severe errors as a result of its effect on the two resource gradients of light and nutrients. As pointed out by Marra et al. (1983), this is a challenge since optical data have often not been collected with the same precision accorded to other variables, such as nutrients.

The nitrate distribution is set by the combination of the input rate, the uptake rate, and the water clarity. We conclude that the observed temporal and spatial variability in nitracline depth and steepness contains a marked optical signature in the coastal upwelling area off Southern California. Our results are primarily derived for the longer temporal and spatial scales, but they also indicate that nitracline dynamics are affected by optics on the shorter temporal and spatial scales, although this point needs to be investigated in dedicated studies. The observed functional relationship between the nitracline depth and the optically transformed chlorophyll concentrations indicates that a primary regulator for the nitrate consumers in this upwelling area is the light limitation induced by the organisms themselves. Although it is not surprising that the nitracline is affected by light attenuation, the high correlations between the nitracline properties and the Secchi depth were surprising. Despite its simplifications, our model provides a mechanistic explanation for these observed correlations. Our results indicate that Secchi disc measurements might serve as a proxy for nitracline properties. Because the Secchi disc came into use more than 100 yr ago (Preisendorfer 1986; Lewis et al. 1988), this can potentially be utilized in reconstruction of nitracline data for time periods and ocean areas in which nutrient measurements are lacking.

References

Aksnes, D. L. 2007. Evidence for visual constraints in large marine fish stocks. Limnol. Oceanogr. **52:** 198–203.

———, and U. Lie. 1990. A coupled physical-biological pelagic model of a shallow sill fjord. Estuar. Coast. Shelf Sci. **31:** 459–486.

Conversi, A., and J. A. McGowan. 1994. Natural versus human-caused variability of water clarity in the Southern California Bight. Limnol. Oceanogr. **39:** 632–648.

Eppley, R. W., E. H. Renger, and W. G. Harrison. 1979. Nitrate and phytoplankton production in Southern California coastal waters. Limnol. Oceanogr. **24:** 483–494.

———, C. Sapienza, and E. H. Renger. 1978. Gradients in phytoplankton stocks and nutrients off Southern California in 1974–76. Estuar. Coast. Mar. Sci. **7:** 291–301.

Fennel, K., and E. Boss. 2003. Subsurface maxima of phytoplankton and chlorophyll: Steady-state solutions from a simple model. Limnol. Oceanogr. **48:** 1521–1534.

Hamre, B., Ø. Frette, S. R. Erga, J. J. Stamnes, and K. Stamnes. 2003. Parameterization and analysis of the optical absorption and scattering coefficients in a western Norwegian fjord: A case II water study. Appl. Optics **42:** 883–892.

Højerslev, N. K., and T. Aarup. 2002. Optical measurements on the Lousiana shelf off the Mississippi river. Estuar. Coast. Shelf Sci. **55:** 599–611.

———, N. Holt, and T. Aarup. 1996. Optical measurements in the North-Sea transition zone. I. On the origin of the deep water in the Kattegat. Cont. Shelf Res. **16:** 1329–1342.

Huisman, J., N. N. P. Thi, D. M. Karl, and B. Sommeijer. 2006. Reduced mixing generates oscillations and chaos in the oceanic deep chlorophyll maximum. Nature **439:** 322–325.

Letelier, R. M., D. M. Karl, M. R. Abbott, and R. B. Bidigare. 2004. Light driven seasonal patterns of chlorophyll and nitrate in the lower euphotic zone of the North Pacific Subtropical Gyre. Limnol. Oceanogr. **49:** 508–519.

Lewis, M. R., W. G. Harrison, N. S. Oakey, D. Herbert, and T. Platt. 1986. Vertical nitrate fluxes in the oligotrophic ocean. Science **234:** 870–873.

———, N. Kuring, and C. Yentsch. 1988. Global patterns of ocean transparency: Implications for the new production of the open ocean. J. Geophys. Res. **93:** 6847–6856.

Lorenzo, E. D. 2003. Seasonal dynamics of the surface circulation in the Southern California current system. Deep-Sea Res. II **50:** 2371–2388.

Marra, J., W. S. Chamberlin, and C. Knudson. 1983. Proportionality between in situ carbon assimilation and bio-optical measures of primary production in the Gulf of Maine in summer. Limnol. Oceanogr. **38:** 232–238.

Morel, A. 1988. Optical modeling of the upper ocean in relation to its biogenous matter content (Case I waters). J. Geophys. Res. **93:** 10749–10768.

Poole, H. H., and W. R. G. Atkins. 1929. Photoelectric measurements of submarine illumination throughout the year. J. Mar. Biol. Assoc. UK **16:** 297–324.

Preisendorfer, R. W. 1986. Secchi disk science: Visual optics of natural waters. Limnol. Oceanogr. **31:** 909–926.

Ryther, J. H. 1956. Photosynthesis in the ocean as a function of light intensity. Limnol. Oceanogr. **1:** 61–69.

Sosa-Ávalos, R., G. Gaxiola-Castro, R. Durazo, and B. G. Mitchell. 2005. Effects on Santa Ana winds on bio-optical properties off Baja California. Cienc. Mar. **31:** 339–348.

Received: 8 June 2006
Accepted: 15 December 2006
Amended: 21 December 2006